Electronic Supplementary Material (ESI) for Industrial Chemistry & Materials.


# Supporting Information

## Hierarchically Ordered Porous Carbon with Atomically Dispersed Cobalt for Oxidative Esterification of Furfural

Wen Yao,[a] Chenghong Hu,[a] Yajie Zhang,[b] Hao Li,[a] Fengliang Wang,[a] Kui Shen,[a] Liyu Chen,[a]* Yingwei Li[a]*

[a] School of Chemistry and Chemical Engineering, South China University of Technology Guangzhou 510640, P.R. China.

[b] State Key Laboratory of Applied Organic Chemistry and Electron Microscopy Centre of Lanzhou University, Lanzhou University, Lanzhou, 730000, P.R. China.

## Experimental Section

### Synthesis of Co-NP/3DOM-NC

The 3D-PS template was immersed into 10 mL of methanol solution containing 4.08 g of $Zn(NO_3)_2 \cdot 6H_2O$, 1g of $Co(acac)_2$ and 3.38 g of 2-MeIM for 2 h, which was then degassed under vacuum for 30 min to assure the precursor solution entered the voids of the template. The obtained 3D-PS@precursor was transferred to a clean beaker and dried at 50 °C overnight. Afterward, the dry 3D-PS@precursor was immersed in a mixed solution of $NH_3 \cdot H_2O/CH_3OH$ (1:1 v/v) and then degassed under vacuum for 30 min to ensure the mixed solution was homogeneously permeated.[2] The above solution was left for complete crystallization for 24 h. $Co(acac)_2$@ZIF-8@PS was obtained after washing with methanol for several times and drying at 50 °C for several hours. Finally, The as-synthesized $Co(acac)_2$@ZIF-8@PS was placed in a tubular furnace and heated to 400 °C with a ramping rate of 5 °C·min$^{-1}$ and kept at 400 °C for 5 h, then to 920 °C with a ramping rate of 5 °C·min$^{-1}$ and kept at 920 °C for 3 h in flowing Ar. The obtained black powders were denoted as Co-NP/3DOM-NC.

### Synthesis of Co-NP/AC

0.5 g of active carbon (AC) was added in 30 mL of $CH_3OH$, and then stirred for 6 h for homogeneous mixing.Then, 245 mg of $Co(NO_3)_2 \cdot 6H_2O$ was dissolved and stirred for 12 h. The above solution was dried in an oven overnight to obtain $Co^{2+}$/AC. Finally, the as-prepared $Co^{2+}$/AC was placed in a tubular furnace and heated to 500 °C with a ramping rate of 5 °C·min$^{-1}$ for 6 h in flowing Ar. The obtained black powders were denoted as Co-NP/AC.

### Characterization

The samples were characterized by scanning electron microscopy (SEM), transmission electron microscopy (TEM), high-resolution transmission electron microscopy (HRTEM), X-ray diffraction (XRD), Raman spectrum, $N_2$ adsorption, and X-ray photoelectron spectroscopy (XPS). X-ray diffraction (XRD) patterns of the samples were recorded on Bruker D8 ADVANCE using Cu Kα radiation (40 kV, 40 mA, λ = 1.543 Å). The 2θ angle of the diffractometer was stepped from 5° to 90° at a

scan rate of 6°/min. Raman spectra were recorded on a LabRAM ARAMIS Raman spectrometer (HORIBA Jobin Yvon). The SEM images were obtained by using a high-resolution field-emission scanning electron microscopy (FESEM, HITACHI SU8220) at the energy of 5 kV. The TEM images were recorded by using a JEM-1400F. HRTEM measurements were performed on JEOL JEM-2100F with EDX analysis (Bruker Xflash 5030T) operated at an accelerating voltage of 200 kV. The $N_2$ adsorption/desorption isotherms were measured by a Micromeritics ASAP 2460 instrument at 77 K. The XPS spectra were obtained on a Thermo ESCALAB 250 spectroscopy at a power of 150 W. The metal contents of the samples were determined by atomic absorption spectroscopy (AAS) on a HITACHI Z-2300 instrument.

The X-ray absorption spectra (XAS) including X-ray absorption near-edge structure (XANES) and extended X-ray absorption fine structure (EXAFS) of the samples at Co K-edge (7709 eV) were collected at the Beijing synchrotron radiation facility (BSRF) center, where a pair of channel-cut Si (111) crystals was used in the monochromator. The Co K-edge XANES data was recorded in a transmission mode. Co foil, $Co_3O_4$, and CoO were used as references. The storage ring was working at the energy of 2.5 GeV with an average electron current of below 200 mA. The acquired EXAFS data were extracted and processed according to the standard procedures using the ATHENA module implemented in the IFEFFIT software packages.

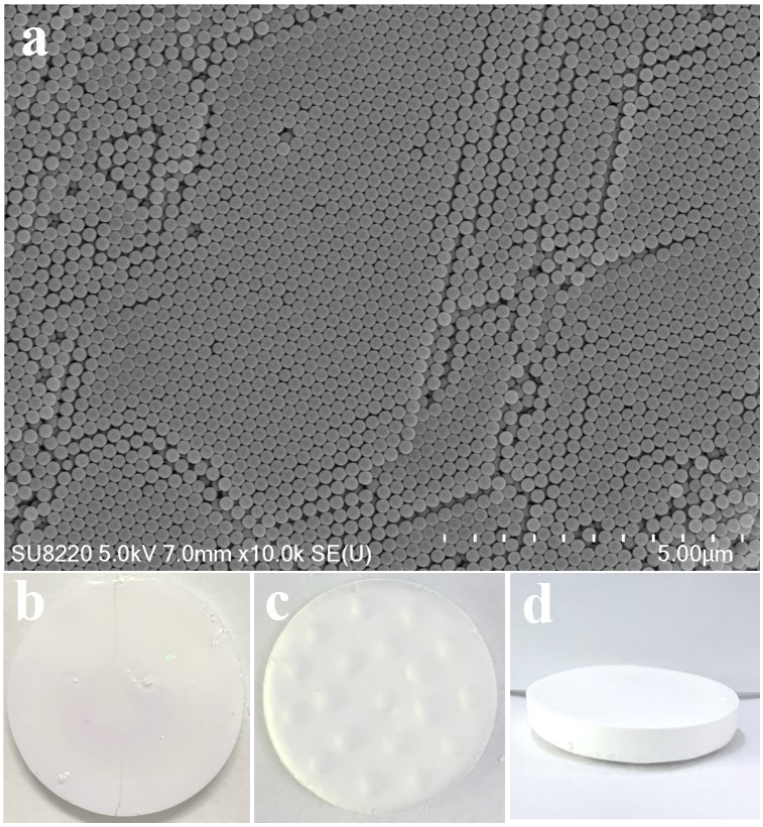


**Figure S1.** (a) SEM image of the monolithic PS template with a size of 210 nm. (b–d) Photographs of bulk PS template.

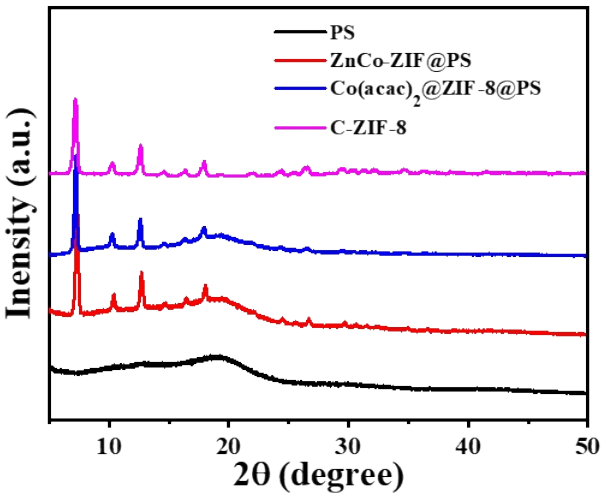


**Figure S2.** XRD patterns of PS, ZnCo-ZIF@PS, $Co(acac)_2$@ZIF-8@PS, and C-ZIF-8.

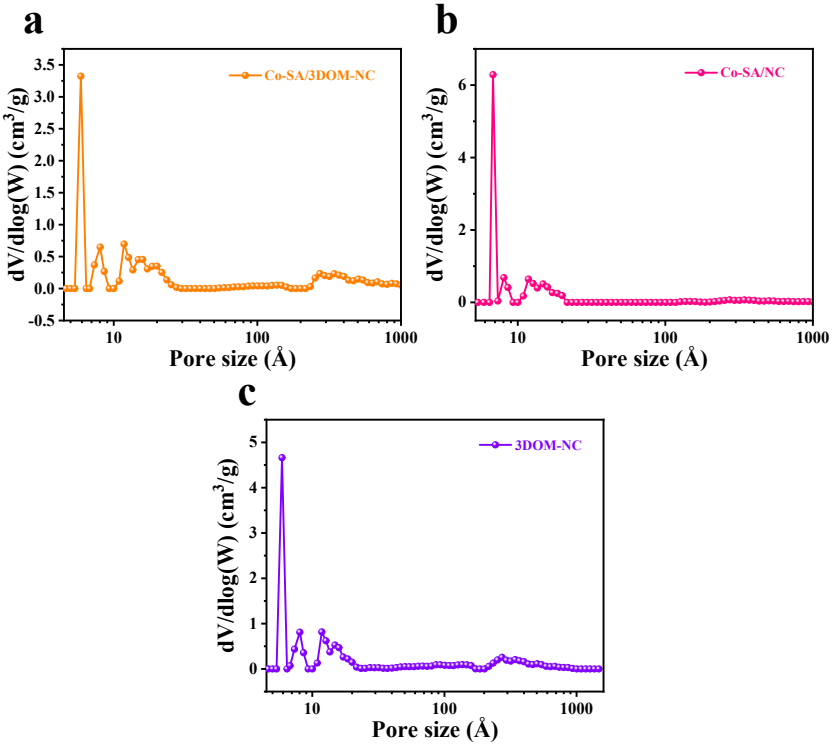


**Figure S3.** Pore-size distributions of (a) Co-SA/3DOM-NC, (b) Co-SA/NC, and (c) 3DOM-NC.

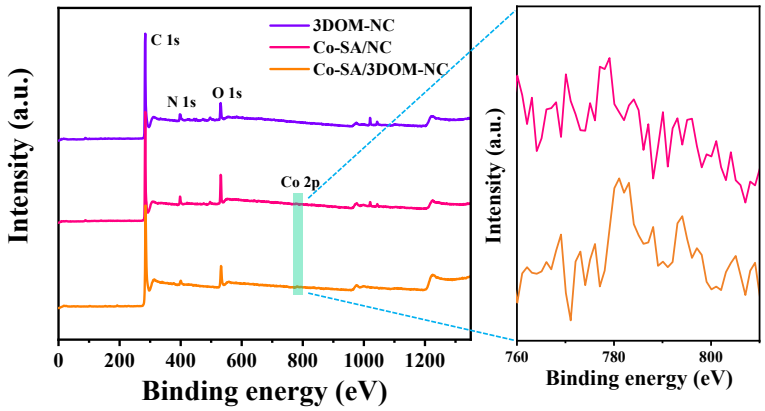


**Figure S4.** XPS survey spectra of Co-SA/3DOM-NC, Co-SA/NC, and 3DOM-NC.

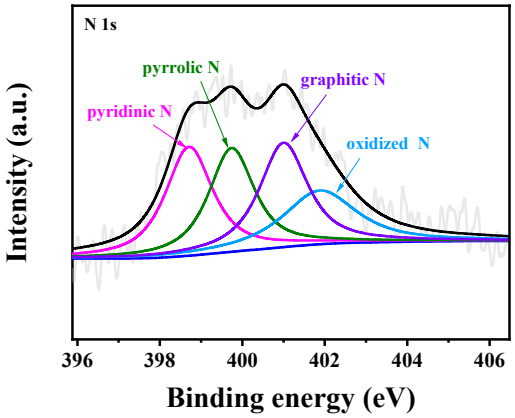


**Figure S5.** High-resolution N1s XPS spectra of Co-SA/3DOM-NC.

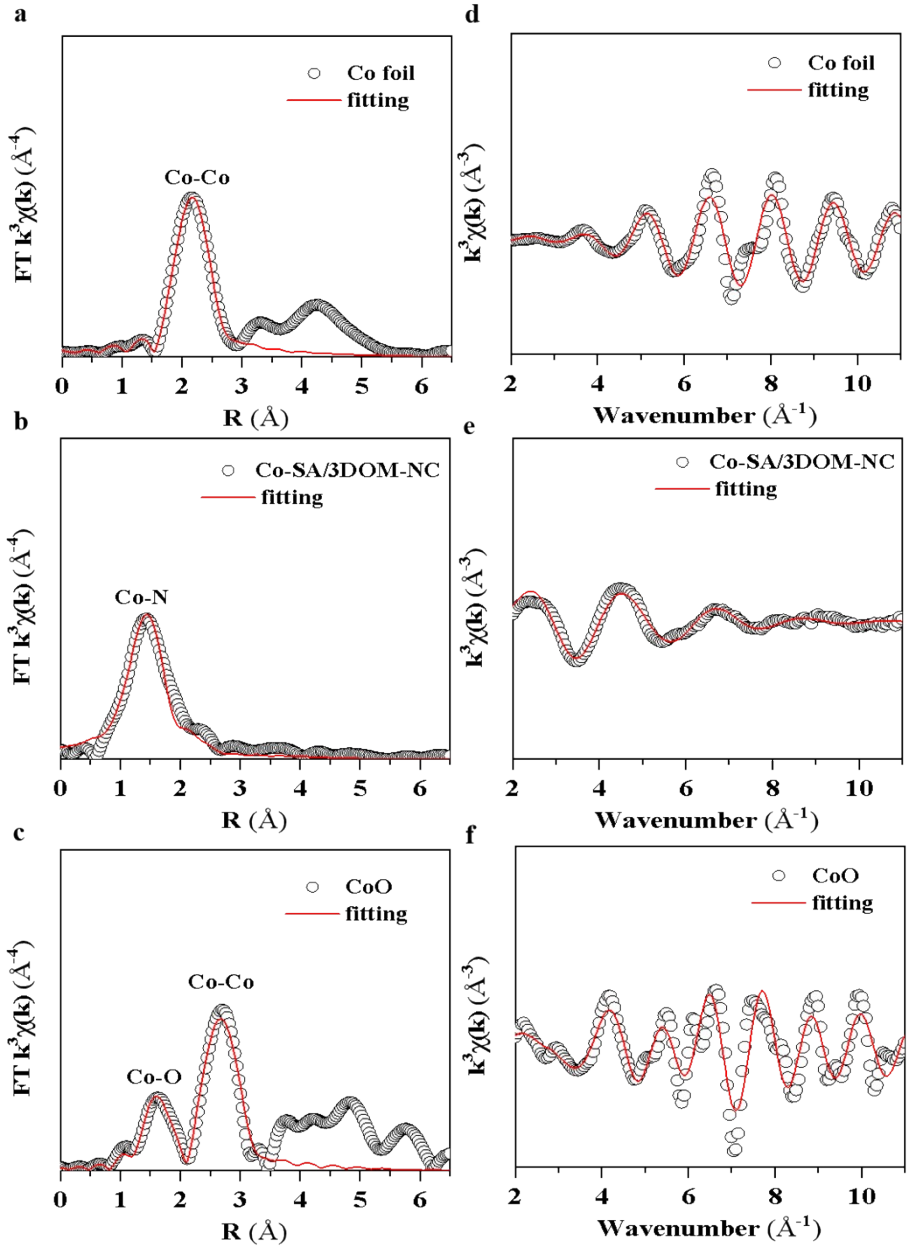


**Figure S6.** (a−c) Corresponding EXAFS fifitting curves at R space for Co-foil, Co-SA/3DOM-NC, and CoO, respectively. (d−f) Wavelet transforms for the $k^3$ weighted EXAFS signals.

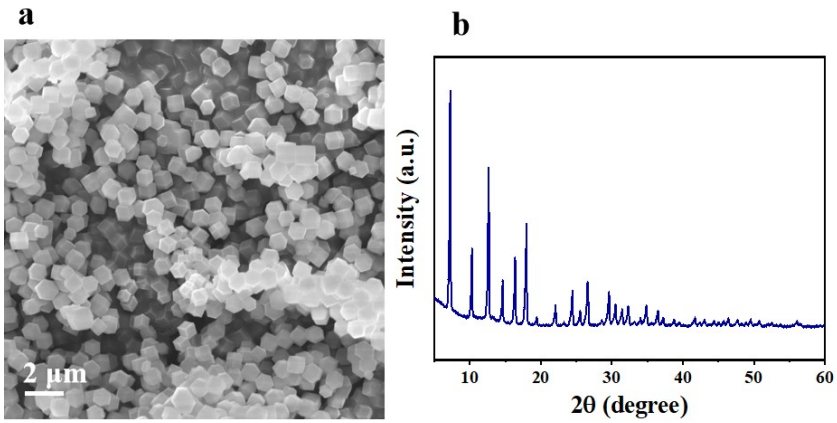


**Figure S7.** (a) SEM image of C-ZnCo-ZIF. (b) XRD pattern of C-ZnCo-ZIF.

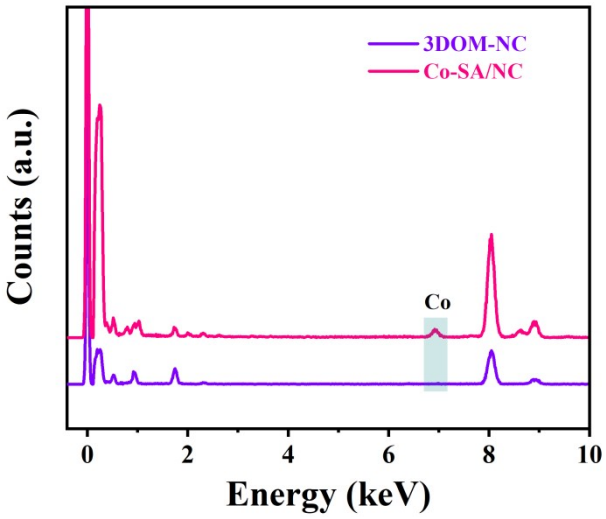


**Figure S8.** EDS spectra of Co-SA/NC and 3DOM-NC.

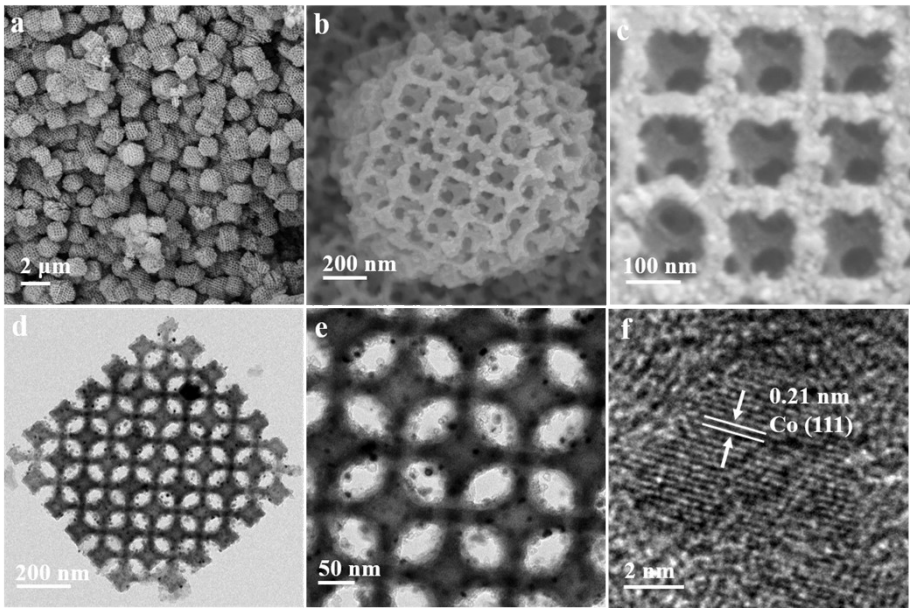


**Figure S9.** (a–c) SEM, (d and e) TEM images and (f) HRTEM image of Co-NP/3DOM-NC.

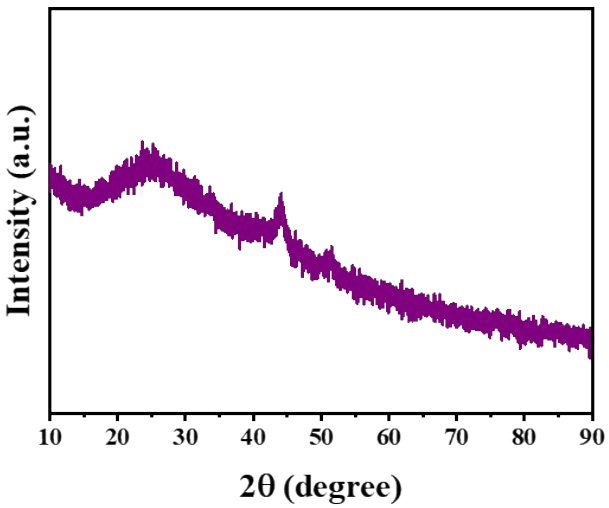


**Figure S10.** XRD patterns of Co-NP/3DOM-NC.

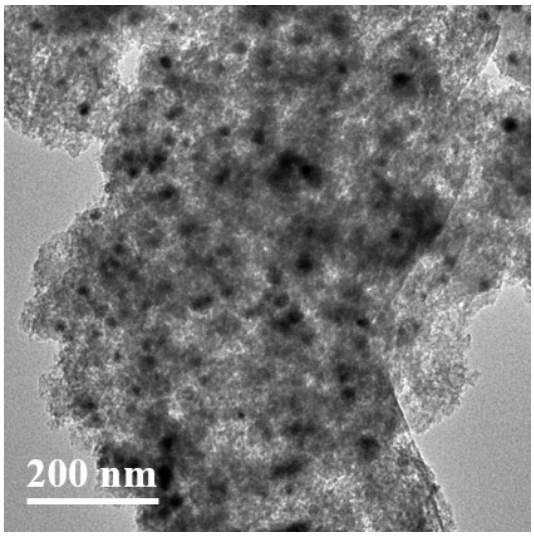


**Figure S11.** TEM image of Co-NP/AC.

**Table S1.** Characterization results of catalysts.

| Samples | Co content (wt%)[a] | Zn content (wt%)[b] | $S_{BET}$ ($m^2/g$) | $S_{Langmuir}$ ($m^2/g$) | $V_{pore}$ ($cm^3/g$) |
|---|---|---|---|---|---|
| Co-SA/3DOM-NC | 1.7 | 3.2 | 708.6 | 1143.0 | 0.43 |
| Co-SA/NC | 1.6 | 3.3 | 772.2 | 1183.6 | 0.44 |
| 3DOM-NC | 0 | 2.8 | 892.4 | 1527.1 | 0.59 |

[a] The Co content is measured by AAS.

[b] The Zn content is measured by ICP-OES.

**Table S2.** EXAFS fitting parameters at the Co K–edge for various samples

| Sample | Shell | *CN*[a] | *R* (Å)[b] | $\sigma^2$ (Å$^2$)[c] | $\Delta E_0$ (eV)[d] | *R* factor |
|---|---|---|---|---|---|---|
| Co foil | Co–Co | 12* | 2.49±0.01 | 0.0060 | 7.9 | 0.0013 |
| CoO | Co–O | 6.0±0.7 | 2.09±0.01 | 0.0072 | 9.8 | 0.0152 |
| | Co–Co | 16.5±2.5 | 3.00±0.01 | 0.0089 | 8.8 | |
| Co-SA/3DOM-NC | Co–N | 3.9±0.9 | 1.95±0.01 | 0.0097 | 5.4 | 0.0178 |

[a] *CN*, coordination number; [b] *R*, distance between absorber and backscatter atoms; [c] $\sigma^2$, Debye-Waller factor to account for both thermal and structural disorders; [d] $\Delta E_0$, inner potential correction; *R* factor indicates the goodness of the fit. $S_0^2$ was fixed to 0.71, according to the experimental EXAFS fit of Co foil by fixing CN as the known crystallographic value. A reasonable range of EXAFS fitting parameters: $0.600 < S_0^2 < 1.000$; $CN > 0$; $\sigma^2 > 0$ Å$^2$; $|\Delta E_0| < 15$ eV; *R* factor < 0.02.

**Table S3.** Effects of stirring speed on the conversion of FFA.

| Stirring speed (r/min) | 300 | 500 | 700 | 900 | 1100 |
|---|---|---|---|---|---|
| Conversion (%) | 90 | 99 | 99 | 98 | 99 |

**Table S4.** Summary of the results of the oxidative esterification of FFA to MF over different catalysts.

| Samples | T (°C) | Additives | $O_2$ pressure (MPa) | Time (h) | Conv. (%) | Sel. (%) | Reference |
|---|---|---|---|---|---|---|---|
| Au/FH | 140 | $K_2CO_3$ | 0.3 | 4 | 46 | 99 | [1] |
| AZ1_400 | 120 | n.a. | 0.6 | 6 | 99 | 100 | [2] |
| $Au_{25}(SG)_{18}/ZrO_2$ | 100 | $Na_2CO_3$ | 0.6 | 3 | 100 | 100 | [3] |
| Au/CMK-3 | 120 | TBHP | 1.0 | 3 | 91.5 | 99 | [4] |
| CoNC/MgO | 120 | n.a. | 0.5 | 6 | 91.4 | 90.0 | [5] |
| $CoO_x$@N-C | 100 | n.a. | 0.5 | 6 | 95 | 97.1 | [6] |
| AZ-500 | 120 | $NaCH_3O$ | 0.6 | 1.5 | 96 | 97 | [7] |
| Zirconia-Au | 120 | n.a. | 0.6 | 1.5 | 82 | 92 | [8] |
| Co@NC (800-2h) | 60 | $K_2CO_3$ | 0.1 | 20 | 100 | 98 | [9] |
| Co-SA/3DOM-NC | 60 | n.a. | 0.1 | 6 | 99 | 100 | This work |

**Table S5.** Oxidative esterification of FFA to MF over different catalysts.

| Samples | Time (h) | T (°C) | P (MPa) | Conversion (%) | MF yield (%) |
|---|---|---|---|---|---|
| [a]- | 6 | 60 | 0.1 | 0 | 0 |
| [a]$Co(NO_3)_2$ | 6 | 60 | 0.1 | 0 | 0 |
| [a]Dimethylimidazole | 6 | 60 | 0.1 | 0 | 0 |
| [a]Co-SA/3DOM-NC | 6 | 60 | 0.1 | 99 | 99 |
| [a]Co-NP/3DOM-NC | 6 | 60 | 0.1 | 24 | 24 |
| [a]Co-SA/NC | 6 | 60 | 0.1 | 18 | 18 |
| [a]Co-NP/AC | 6 | 60 | 0.1 | 0 | 0 |
| [a]AC | 6 | 60 | 0.1 | 0 | 0 |
| [b]Co-SA/3DOM-NC | 6 | 60 | 0.1 | 21 | 21 |
| [c]Co-SA/3DOM-NC | 6 | 60 | 0.1 | 5 | 5 |
| [d]Co-SA/3DOM-NC | 6 | 60 | 0.1 | 36 | 36 |

[a]Standard reaction conditions: 0.1 mmol FFA, 1.0 mL $CH_3OH$, $O_2$ balloon (1.0 bar), 60 °C.

[b] Adding 1.0 equiv. KSCN.

[c] In the absence of $O_2$.

[d] In the presence of BHT.

**Reference**


[1] X. Tong, Z. Liu, L. Yua, Y. Li, A tunable process: catalytic transformation of renewable furfural with aliphatic alcohols in the presence of molecular oxygen, *Chem. Commun.,* 2015, **51**, 3674–3677.

[2] C. Ampelli, G. Centi, C. Genovese, G. Papanikolaou, R. Pizzi, S. Perathoner, R.-J. van Putten, K. J. P. Schouten, A. C. Gluhoi, J. C. van der Waa, A Comparative Catalyst Evaluation for the Selective Oxidative Esterification of Furfural, *Top Catal.,* 2016, **59**, 1659–1667.

[3] Z. Shahin, F. Rataboul, A. Demessence. Study of the oxidative esterifcation of furfural catalyzed by $Au_{25}$(glutathione)$_{18}$ nanocluster deposited on zirconia, *Mol. Catal.,* 2021, **499**, 111265.

[4] R. Radhakrishnan, S. Thiripuranthagan, A. Devarajan, S. Kumaravel, E. Erusappan, K. Kannan, Oxidative esterification of furfural by Au nanoparticles supported CMK-3 mesoporous catalysts, *Appl. Catal. A-Gen.* 2017, **545**, 33–43.

[5] N. Huo, H. Ma, X. Wang, T. Wang, G. Wang , T. Wang, L. Hou, J. Gao, J. Xu, High-efficiency oxidative esterification of furfural to methylfuroate with a non-precious metal Co-N-C/MgO catalyst, *Chinese J. Catal.* 2017, **38**, 1148–1154.

[6] T. Wang, H. Ma, X. Liu, Y. Luo, S. Zhang, Y. Sun, X. Wang, J. Gao, J. Xu, Ultrahigh-Content Nitrogen-doped Carbon Encapsulating Cobalt NPs as Catalyst for Oxidative Esterification of Furfural, *Chem. Asian J.* 2019, 14, 1515–1522.

[7] M. Signoretto, F. Menegazzo, L. Contessotto, F. Pinna, M. Manzoli, F. Boccuzzi, Au/ZrO2: an efficient and reusable catalyst for the oxidative esterification of renewable furfural, *Appl. Catal. B-Environ.,* 2013, **129**, 287–293.

[8] F. Menegazzo, M. Signoretto, F. Pinna, M. Manzoli, V. Aina,G. Cerrat, F. Boccuzzi, Oxidative esterification of renewable furfural on gold-based catalysts: Which is the best support?, *J. Catal.,* 2014, **309**, 241–247.

[9] F. Mao, Z. Qi, H. Fan, D. Sui, R. Chen, J. Huang, Heterogeneous cobalt catalysts for selective oxygenation of alcohols to aldehydes, esters and nitriles, *RSC Adv.,* 2017, **7**, 1498–1503.